Overexpression of the ABA-responsive transcription factor PtrMYBH alters shoot apical meristem, xylem, root, and leaf development in *Populus*

Ziqi Liu[1,†], Xiaomeng Fan[2,†], Xuqing Liu[1,†], Zeyu Zhang[1,†], Xiangrong Li[2], Yingjie Yan[2], Shengcai Xiang[2], Xiaoqi Zhang[3], Tingting Lu[3], Siyu Lu[3], Dengcan Liu[2], Tian Hua[2], Mengna Zhao[2], Jun Zhang[2], Hangxiao Zhang[2] and Lianfeng Gu[2,*] [iD]

[1]*College of Forestry, Fujian Agriculture and Forestry University, Fuzhou 350002, China,*

[2]*Fujian Provincial Key Laboratory of Haixia Applied Plant Systems Biology, Basic Forestry and Proteomics Research Center, School of Future Technology, Haixia Institute of Science and Technology, Fujian Agriculture and Forestry University, Fuzhou 350002, China, and*

[3]*College of Life Sciences, Fujian Agriculture and Forestry University, Fuzhou 350002, China*

SUMMARY

Abscisic acid (ABA) mediates stress responses and growth regulation in plants, but the roles of ABA-responsive transcription factors (TFs) in *Populus* development remain poorly characterized. Here, we identified an ABA-upregulated TF and investigated its function through overexpression in transgenic poplar. The *PtrMYBH* is upregulated during ABA treatment, and its overexpression in transgenic poplar leads to leaf malformations, including reduced size and curling, with severity correlating with *PtrMYBH*-overexpression levels in three independent transgenic lines. *PtrMYBH* regulates stomatal growth and development, resulting in decreased stomatal length and aperture, along with distinct leaf structural abnormalities. Additionally, *PtrMYBH* affects root development, with overexpressing lines showing an increase in adventitious root number but shorter lengths, alongside morphological changes in the root elongation zone. Furthermore, morphological changes are observed in the shoot apical meristem (SAM) and stem-differentiating xylem (SDX) of *PtrMYBH*-overexpressing poplar. RNA-seq analyses reveal *PtrMYBH*'s influence on the expression of genes related to cellular proliferation in the SAM and developmental pathways in the SDX. Finally, in *PtrMYBH*-overexpressing lines, ABA treatment results in leaf tip damage, earlier leaf drop, and stunted growth, highlighting its critical role in the ABA response. These findings lay a foundation for further exploration of TFs like *PtrMYBH* to regulate growth in *Populus* species.

Keywords: abscisic acid, leaves development, *Populus trichocarpa*, shoot tip, stem-differentiating xylem.

INTRODUCTION

The phytohormone abscisic acid (ABA), first investigated in the 1960s, plays a crucial role throughout the entire lifecycle of plants (Leung & Giraudat, 1998). It regulates physiological processes, such as growth, stomatal aperture, hydraulic conductivity, and seed dormancy, as well as mediating responses to biotic and abiotic stresses (Ali et al., 2022; Leung & Giraudat, 1998; Raghavendra et al., 2010). ABA is generally regarded as a growth inhibitor, as high concentrations of exogenously applied ABA inhibit root growth (Luo et al., 2014; Sun et al., 2018) and endogenous ABA accumulates significantly in plants subjected to abiotic stress (Cramer & Quarrie, 2002). On the other hand, gene editing of ABA receptors has been shown

to improve plant growth and yield (Miao et al., 2018; Yoshida et al., 2019). Contrary to the widely accepted notion of ABA as a growth inhibitor, some studies suggest that ABA can also stimulate plant growth and development. For example, mutants deficient in endogenous ABA exhibit impaired vegetative growth, which can be improved with the application of exogenous ABA (Barrero et al., 2005; Humplík et al., 2017).

Several transcription factor families, including basic leucine zipper (bZIP), Myeloblastosis (MYB), *Apetala*2/ ethylene-responsive element binding factor (AP2/ERF), homeodomain-leucine zipper (HD-ZIP), NAM/ATAF/CUP (NAC), and basic helix–loop–helix (bHLH), among others, play critical roles in mediating ABA responses and

regulating gene expression in plants (Chen et al., 2020; Cutler et al., 2010). The MYB transcription factor family is one of the largest in plants and is characterized by having one to four imperfect repeats (R) and each with 50–53 residues encoding three α-helices. MYB factors are classified into four groups based on the number and arrangement of their MYB domains: 1R (MYB-related and others), 2R (R2R3-MYB), 3R (R1R2R3-MYB), and 4R (four R1/R2-like repeats). MYB genes are far more numerous in plants compared with fungi or animals and are crucial for various processes including primary and secondary metabolism, cell fate and identity, developmental processes, and responses to biotic and abiotic stresses (Chen et al., 2006; Dubos et al., 2010; Liu et al., 2015).

Numerous studies have demonstrated that MYB plays a crucial role in the ABA signaling pathway, influencing plant growth and development throughout its life cycle. For example, in *Arabidopsis*, *MYB101* and *MYB33* are regulated by miR159, which affects their role in seed germination through ABA responses (Reyes & Chua, 2007). Overexpression of *AtMYBL*, a member of the MYB-related gene family, results in a marked leaf senescence phenotype and is regulated by ABA (Zhang et al., 2010). Additionally, MYB74, a member of the R2R3-MYB protein family in *Arabidopsis*, modulates plant growth by affecting *MYB11* and *MYB77* through an ABA-dependent pathway. MYB74 activates *MYB11*, which delays meristematic cell proliferation, and represses *MYB77*, which impairs lateral root formation, leading to significant growth inhibition (Ortiz-García et al., 2022). Furthermore, the role of MYB in regulating plant growth and development via the ABA-dependent pathway has been observed in rice (Zhu et al., 2015), tomato (Zhang et al., 2023), maize (Zhai et al., 2020), potato (Sun et al., 2019), pummelo (Shi et al., 2020), and citrus (Zhang et al., 2023).

In poplar, some studies have explored how MYB regulates responses to biotic and abiotic stresses (Long et al., 2024; Plett et al., 2010; Yang, Cortijo, et al., 2021). Moreover, several MYB transcription factors (TFs) have been shown to act as repressors or activators influencing secondary cell wall (SCW) biosynthesis (Jiang et al., 2022; Jiao et al., 2019; Tang et al., 2023). *PeMYB33* in poplar negatively regulates the formation of adventitious roots by participating in the ABA signaling pathway (Zhao et al., 2024). Despite these findings, the role of MYB in regulating growth and development in woody plants is still not well understood. Given poplar's high genetic diversity and rapid growth, further in-depth research into growth and developmental mechanisms is highly valuable (Ko et al., 2011; Stolarski et al., 2024).

In this study, *PtrMYBH*, a MYB-related gene, was identified by analyzing differentially expressed genes (DEGs) in *Populus trichocarpa* (*P. trichocarpa*) treated with ABA. Stable overexpression of *PtrMYBH* in *Populus alba* "Berolinensis" resulted in dwarf phenotypes with curled leaves and localized necrosis. Additionally, three gradually increasing levels of *PtrMYBH* overexpression in three independent transgenic lines corresponded to increasingly severe phenotypic changes. Exogenous ABA treatment suppressed growth in both *OE-MYBH* and wild-type (WT) plants, leading to increased *PtrMYBH* expression and similar phenotypes to those observed in *OE-MYBH* plants. Taken together, these results suggest that *PtrMYBH* inhibits plant growth and development through an ABA-dependent pathway. Overall, *PtrMYBH* appears to function as a negative regulator of growth and development in poplar.

RESULTS

Differentially expressed genes (DEGs) in response to ABA stress in different tissues

To comprehensively investigate the transcriptome of *P. trichocarpa* during the ABA response, we sequenced 36 mRNA samples from SDX, phloem, shoot tip, and leaves exposed to ABA treatments at 0, 24, and 48 h (Figure 1a). The sequencing was performed using rRNA-depleted dUTP method on Illumina Hiseq2500 platform, yielding a total of 936 533 116 paired-end reads to calculate gene expression and DEGs (Tables S2 and S3). First, we analyzed tissue-specific gene expression patterns in *P. trichocarpa* across four tissues. Our results revealed that the number of tissue-specific highly expressed genes was 3264, 4179, 5019, and 3852 for leaf, shoot tip, phloem, and xylem, respectively (Figure 1b; Table S4). We performed GO enrichment analysis on tissue-specifically expressed genes (Figure S1, Table S5). Leaf-highly expressed genes significantly enriched ($P < 0.05$) in GO terms such as photosynthesis, chlorophyll biosynthetic process, electron transport chain, and chloroplast organization. Shoot tip-highly expressed genes are primarily associated with maintenance of plant organ identity, DNA replication initiation, and Group II intron splicing. Phloem-highly expressed genes are notably involved in callose deposition in phloem sieve plate, with additional enrichment observed in host immune response terms. Xylem-highly expressed genes are linked to cell wall biogenesis, cell wall organization, and hemicellulose metabolic process.

Next, we examined whether these tissue-specific genes responded to ABA treatment. Based on their expression changes following ABA treatment, we classified them into five distinct clusters, each representing a unique expression trend (Figure 1c, Tables S6).

In leaves, ABA-responsive GO terms were predominantly enriched in photosynthesis (Figure S2, Table S10). Notably, we identified significant enrichment of cell redox homeostasis terms. In shoot tips, enriched GO terms included ribosomal biogenesis, nucleosome binding, and
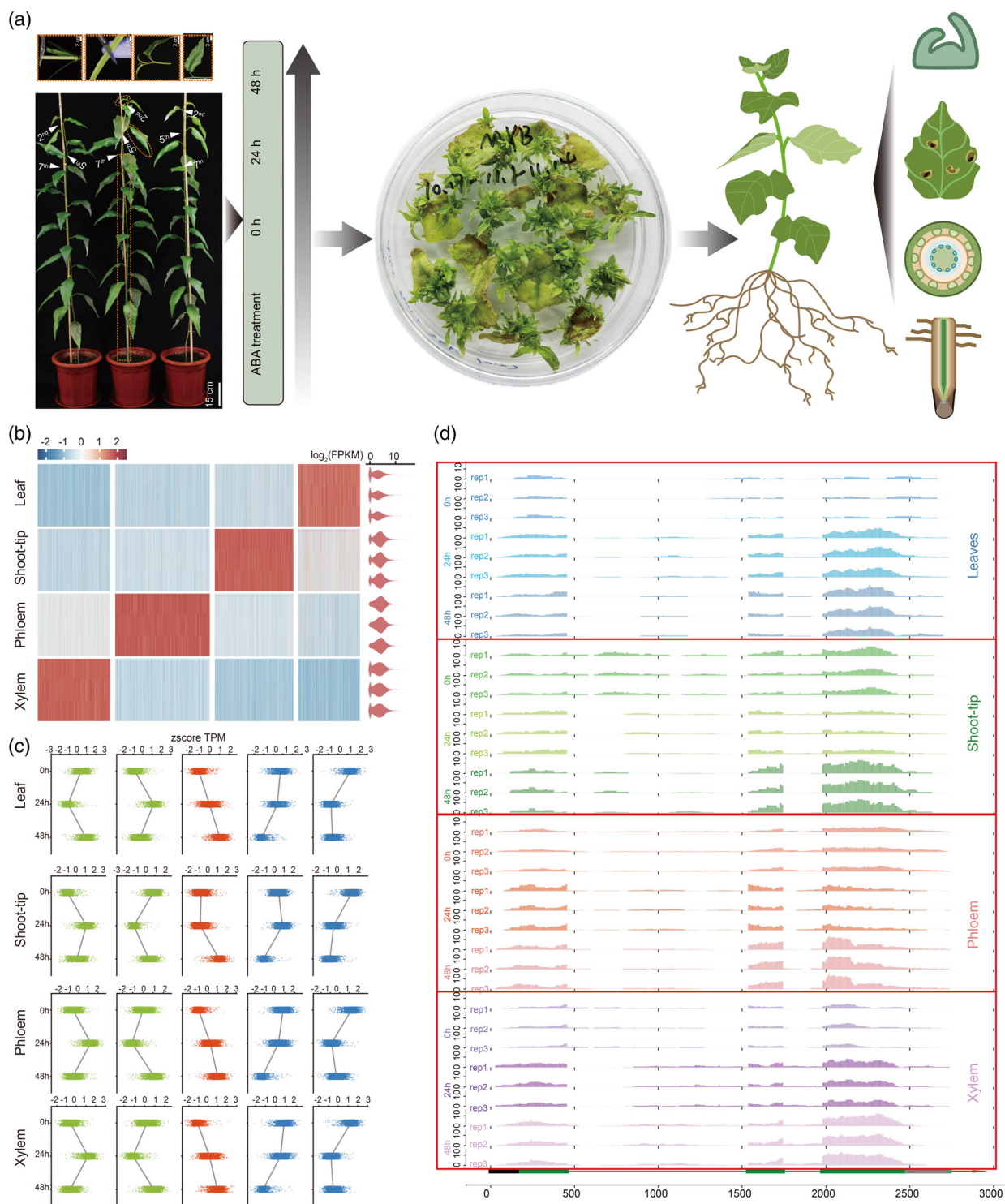
Figure 1. The impact of ABA treatment on gene expression in xylem, phloem, leaf, and shoot tip.
(a) Schematic representation of the experimental workflow: ABA treatment at 0, 24, and 48 h, differential gene expression analysis in four tissues (xylem, phloem, leaf, and shoot tip), and the construction of *PtrMYBH*-overexpressing transgenic poplars to assess its impact on growth and development from SAM, SDX, leaves, and roots.
(b) Heatmap presented tissue-specific gene expression patterns.
(c) clustering analysis of ABA-responsive genes across four tissues. DEGs (|FC| ≥ 2, $P < 0.05$) were identified for each tissue type. Data were *z*-score normalized (scipy v1.10.1) and clustered via K-means (sklearn v1.2.2).
(d) Wiggle plots showing upregulated gene expression of *PtrMYBH* across different tissues under ABA treatment.

DNA replication (Figure S3, Table S11), aligning with this tissue's proliferative capacity. In xylem, ABA-responsive terms were strongly biased toward cell wall biogenesis, with enrichments in lignin biosynthesis, cellulose metabolism, and hemicellulose metabolism (Figure S4, Table S12), consistent with regulation in secondary xylem development. In phloem, beyond expected enrichments in callose deposition and phloem development, ABA-responsive genes were uniquely enriched in systemic acquired resistance and oxidoreductase activity (Figure S5, Table S13), suggesting potential relation with redox.

OE-PtrMYBH leads to leaf malformation of *P. Alba* "Berolinensis"

All genes with TFs annotation were identified using eggNOG-mapper, followed by intersection analysis with ABA-responsive genes (Table S14). MYB and AP-family TFs showed the highest representation among ABA-response TFs, particularly in shoot tip (Figure S6A). We identified an ABA-related gene, *PtrMYBH* (Potri.003G079500), that is significantly upregulated across different tissues under ABA stress treatment (Figure S7). This gene exhibited both high basal expression across tissue and ABA-inducibility (Figure 1d; Figure S6B). Consistent with the RNA-seq results, reverse transcription quantitative PCR (RT-qPCR) analysis confirmed the expression levels in the phloem, xylem, leaf, and shoot tip under 0, 24, and 48 h ABA treatment observed in the RNA-seq (Figure 2a).

We overexpressed *PtrMYBH* in *P. alba* "Berolinensis" to generate transgenic overexpression lines, obtaining three independent lines designated as *OE-MYBH* (*49-7*), *OE-MYBH* (*84-3*), and *OE-MYBH* (*84-4*) (Figure 2b). Significant changes in leaf morphology were observed in the *PtrMYBH*-overexpression lines. The leaves of 2-month-old *OE-MYBH* (*49-7*) and *OE-MYBH* (*84-3*) plants were smaller than those of the WT, showing pronounced curling and localized necrosis, whereas the leaves of *OE-MYBH* (*84-4*) showed only slight curling (Figure 2c). Additionally, RT-qPCR analysis showed that *PtrMYBH* expression levels were increased by 35.728-, 24.412-, and 4.486-fold in the *OE-MYBH* (*49-7*), *OE-MYBH* (*84-3*), and *OE-MYBH* (*84-4*) lines, respectively (Figure 2d). Therefore, the degree of leaf curling corresponds directly to the level of *PtrMYBH* overexpression. The *OE-MYBH* (*84-4*) line, due to its lower level of overexpression, does not exhibit a pronounced leaf curling phenotype; however, it does show a noticeable increase in leaf size (Figure 2e).

Since we identified the enrichment of cell redox homeostasis and oxidoreductase activity (Figures S3 and S5), we investigated the analysis of reactive oxygen species (ROS) levels in *PtrMYBH* overexpression. We conducted histochemical staining to compare the level of two major ROS components H_2O_2 and O_2^- between WT and three MYBH-overexpression lines (Figure 2f). In NBT staining assays, two overexpression lines (*OE-MYBH 49-7 and 84-3*) displayed stronger blue coloration compared with WT, demonstrating elevated O_2^- levels. The DAB staining results showed that overexpression lines exhibited slightly deeper staining intensity compared with WT, accompanied by faint yellowish-brown speckles. We further quantified H_2O_2 content in leaves of *OE-MYBH* transgenic lines and WT control using the Hydrogen Peroxide Content Assay Kit. The results revealed that *OE-MYBH* lines (*OE-MYBH 84-3 and 84-4*) exhibited higher H_2O_2 levels compared with WT (Figure S7A), suggesting that *PtrMYBH* overexpression likely contributed to the modulation of ROS accumulation. According to RNA-seq results, we also observed a general upregulation of genes with peroxidase activity in *OE-MYBH* lines compared with WT (Figure S7B). Peroxidase genes presented elevated expression levels in *OE-MYBH* transgenic lines (Figure S7C,D). These findings further supported the role of *PtrMYBH* in modulating oxidative stress responses.

PrtMYBH regulates the size of stomata

Stomata are crucial for maintaining water balance, serving as the primary interface between plants and their environment. Leaf discs (1 cm) were prepared using a perforator and underwent fixation, decolorization, and transparency treatment. Stomatal closure was assessed using a fluorescence inverted microscope (Figure 3a). The stomata of the leaves were observed under 40× magnification. Our analysis of stomatal morphology revealed distinct phenotypic alterations in transgenic lines compared with WT controls. We investigated stomatal length (Figure 3b), aperture (Figure 3c), and density (Figure 3d) and found that stomatal length and aperture were promoted in line 84-4. Stomatal aperture was suppressed in

**Figure 2.** Overexpression of *PtrMYBH* in *P. alba* "Berolinensis" results in leaf Malformation.

(a) Expression level of *PtrMYBH* under 0, 24, and 48 h ABA treatment in four tissues. Values are means ± SD, $n = 3$, *$P < 0.05$, **$P < 0.01$, ***$P < 0.001$, ****$P < 0.0001$. Student's *t*-test.

(b) The whole-plant phenotype images of 35-day-old WT, *OE-MYBH* (*49–7*), *OE-MYBH* (*84–3*), and *OE-MYBH* (*84–4*) plants, respectively. Scale bars of plants, 10 cm. Scale bars of 13th leaves, 5 cm.

(c) Phenotype of the first fully unfolded leaf to the 21st leaf of the WT and *OE-MYBH* (Scale bar = 10 cm).

(d) The expression levels of *PtrMYBH* in WT and *OE-MYBH* (*49–7, 84–3*, and *84–4*) lines were detected by real-time quantitative RT-PCR. Values are means ± SD, $n = 3$, ***$P < 0.001$, ****$P < 0.0001$. One-way ANOVA with Dunnett's test.

(e) Measurements of leaf area.

(f) Histochemical staining using DAB and NBT on leaves of WT and *OE-MYBH* lines.
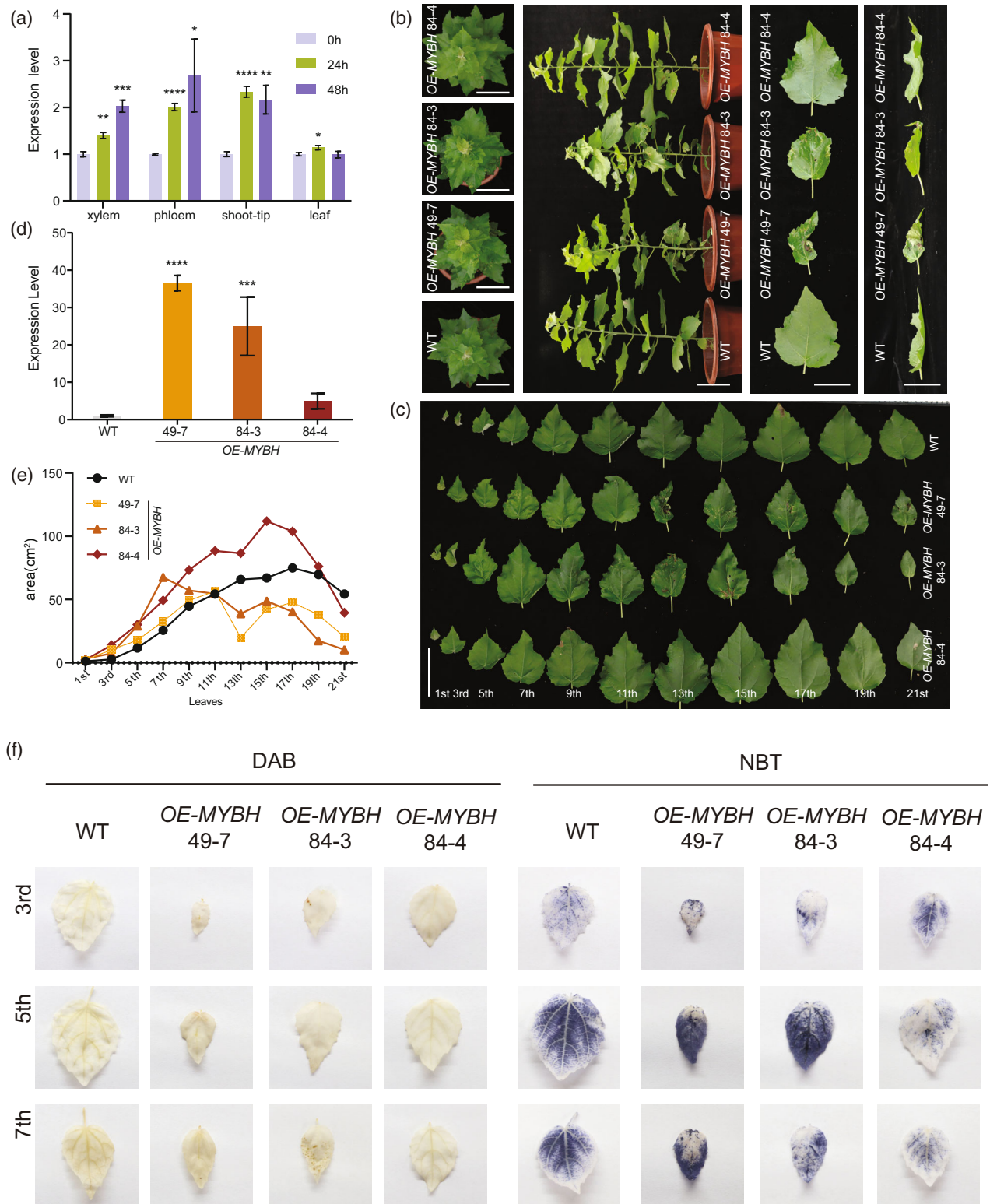
both line 49-7 and line 84-3. No statistically significant differences were found in stomatal density among all tested lines. Examining longitudinal sections of the leaves

revealed significant differences in leaf tissue structure among *PtrMYBH*-overexpression lines (49-7, 84-3, and 84-4) compared with the WT (Figure 3e). Specifically, the
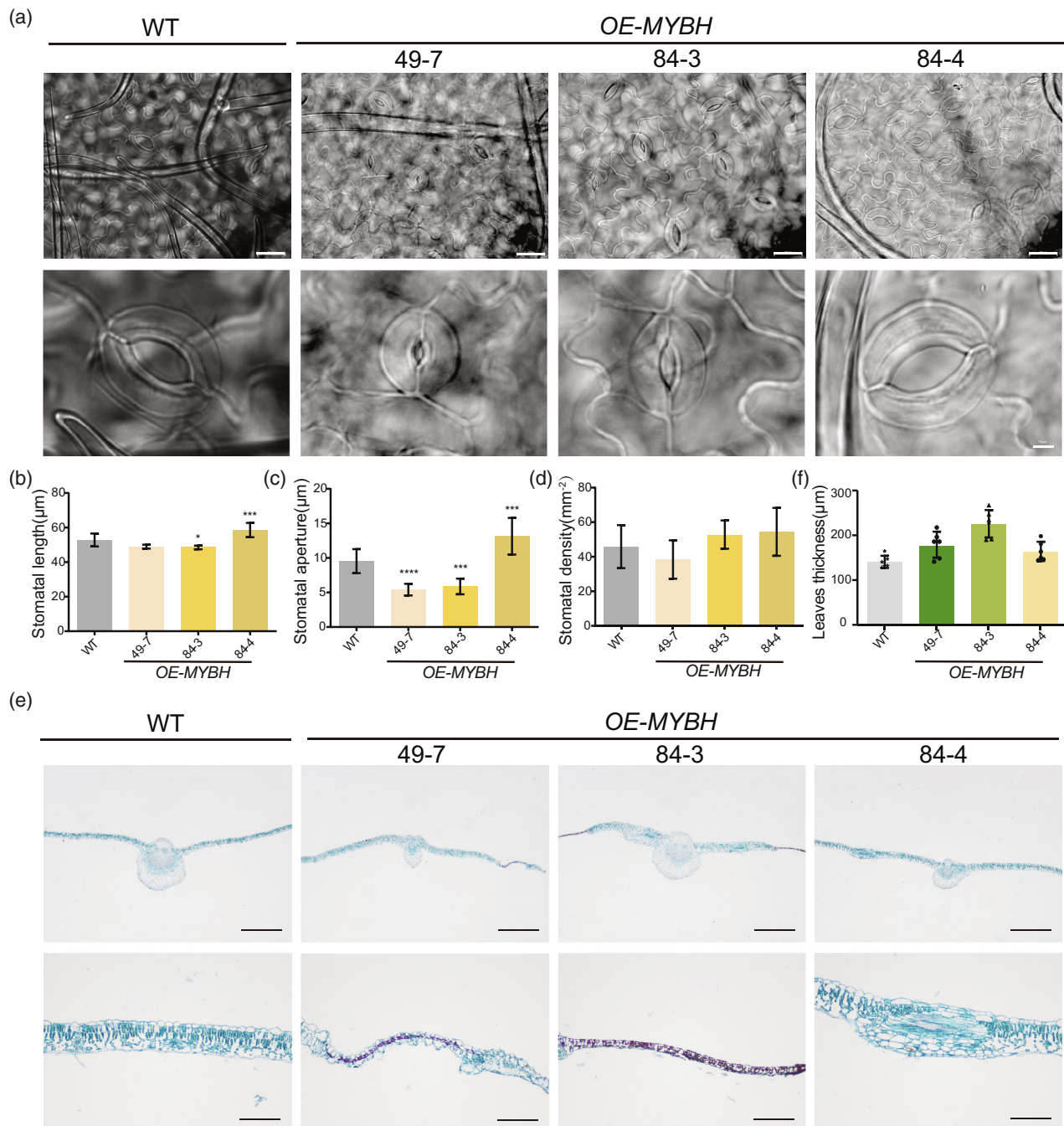
Figure 3. Leaf stomatal and longitudinal section cytological slices in *OE-MYBH*.
(a) Images of stomata (scale bar = 50 µm) and the enlarged detail (scale bar = 10 µm).
(b) The bar chart shows the length of stomata.
(c) The bar chart shows stomatal aperture.
(d) The bar chart shows stomata density.
(e) Leaf longitudinal section (scale bar = 1000 µm) and the enlarged detail (scale bar = 200 µm).
(f) The bar chart shows leaf width. Data represent the means ± SD of six independent biological samples of *OE-MYBH* and six biological samples of WT, respectively. $*P < 0.05$, $***P < 0.001$, $****P < 0.0001$. One-way ANOVA with Dunnett's test.

leaves of the overexpression lines exhibited distinct lesions under the microscope, characterized by localized disorganization of cellular structures. Furthermore, precise measurements of leaf thickness revealed that the average leaf thickness in *PtrMYBH*-overexpression lines was greater than that of the WT (Figure 3f).

PrtMYBH affects root growth and development

Roots are a crucial part of plants, serving as the foundation for growth and adaptation to the environment. Lateral branches (8 cm) of *OE-MYBH* were cut and induced to grow adventitious roots in a rooting solution. After 1 month, the roots were photographed, recorded, and measured using ImageJ (Figure 4a). The *OE-MYBH* lines produced approximately 10 adventitious roots, averaging 5–6 more than WT. Statistical analysis revealed that line 84–3 presented significant increases in the amount of adventitious root compared with WT (Figure 4b). The root length of the *OE-MYBH* lines ranged from 0.3 to 6.9 cm, mainly between 2 and 5 cm, which is shorter than that of WT roots, which ranged from 1 to 11 cm (Figure 4c). After 1 month of cultivation in soil, the two strains with higher *PtrMYBH* overexpression (*49–7* and *84–3*) showed a 50% reduction in the length of the longest root compared with the WT. In contrast, the longest root of *OE-MYBH* (*84–4*), with the lowest level of *MYBH* overexpression, was slightly longer than that of the WT. Measurements of the root elongation zone showed that the width in WT roots was 2–3 times greater than that of the overexpressing strains. The width of the root elongation zone presented a significant reduction in *OE-MYBH* (49–7, 84–3, and 84–4) compared with WT (Figure 4d). Analysis of root tip sections revealed significant morphology changes in the *OE-MYBH* strains compared with the WT (Figure 4e).

Morphological and transcriptome analysis of SAM and SDX segments in *OE-MYBH*

In the comparative morphological analyses of *OE-MYBH*- and WT SAM, significant morphological changes were observed. The *OE-MYBH* SAM appeared narrower and sharper, suggesting a reduction in the cell proliferation area (Figure 5a). Measurement and statistical analyses of SDX sections revealed that the width and proportion of xylem in the stem varied with *PtrMYBH* expression levels (Figure 5b). Compared with WT, the 49–7 line (with highest *PtrMYBH* expression) exhibited significantly increased xylem width (Figure 5c) and amount (Figure 5d), with higher expression levels associated with increased xylem width and quantity. For example, the *PtrMYBH 49–7* lines exhibited the highest xylem width and amount. To further dissect the role of *PrtMYBHPtrMYBH* in growth and development regulation, we conducted RNA-seq on SDX and shoot tips of WT and *OE-MYBH* samples. GO enrichment analysis of downregulated genes in the SAM indicated involvement in processes related to the pentose phosphate pathway, glucose 6-phosphate metabolism, glyceraldehyde-3-phosphate metabolism, and carbohydrate metabolism. The GO enrichment analysis of upregulated genes in SAM reveals the activation of pathways related to RNA destabilization, including genes linked to

the mRNA catabolic process. Additionally, the upregulated genes also participated in the raffinose family oligosaccharide biosynthetic process and Notch signaling pathway. Downregulation in SDX highlighted a reduction in pathways involved in cell division, chitin response, and phloem or xylem histogenesis. Conversely, the upregulated GO enrichment analysis showed enhanced pathways related to protein localization to the membrane, negative regulation of protein catabolic processes, and manganese ion transport.

Compared with WT, the terminal buds of the *OE-MYBH*-overexpression lines become smaller and more pointed with increasing *MYBH* expression levels. Through transcriptomic analysis of SAM and SDX, we identified DEGs in the tip bud materials from the *MYBH*-overexpression lines (Figure 5e). Based on GO annotation using eggNOG-mapper (v2.1.12), we focused on several meristem-related genes: *PabRPs* (GO:0010014, meristem initiation), *PabEP* (GO:0048507, meristem development), *PabMLP* (GO:0010228, vegetative to reproductive phase transition), and *PabBARD1* (GO:0010492, maintenance of SAM). We used qPCR to further verify four genes related to SAM. The expression levels of these four genes showed consistent gradient changes corresponding to the varying degrees of *MYBH* overexpression. These SAM-related genes were significantly increased in the *OE-MYBH* (*49–7*, *84–3*, and *84–4*) potentially affecting cell division of SAM.

The width and proportion of xylem were significantly increased in the 49–7 lines with high *MYBH* expression. We selected four genes associated with stem-differentiating xylem development: *PabERF105*, *PabHPc*, *PabIAA13B*, and *PabIAA13C*. Through qPCR validation, we found that these four SDX-related genes were upregulated in line 49–7 but downregulated in lines 84–3 and 84–4 compared with WT (Figure 5f). In poplar, *PagERF81* belongs to the AP2/ERF superfamily and plays an important role in the regulation of lignin and fiber cells in xylem (Zhao et al., 2023). In MYBH-overexpression lines, *ERF105* was significantly upregulated in SDX, coinciding with anatomical changes in xylem morphology (Figure 5a). Given the conserved roles of AP2/ERF members in xylogenesis (Zhao et al., 2023), we propose that the upregulation of *ERF105* in *MYBH*-overexpression lines may affect the development of xylem. However, the hypothesis should be validated in future studies through transgenic assays.

Auxin controls the stability of Aux/IAA9 protein, thereby affecting the expression of HD-ZIP III gene, and ultimately regulates the differentiation of xylem (Xu et al., 2019). IAA13C and IAA13B are two auxin-responsive proteins. We observed the regulation of these two genes in the *OE-MYBH* lines. Therefore, the upregulation of *IAA13C* and *IAA13B* in the *MYBH*-overexpression line may regulate the xylem development through the auxin signaling pathway.
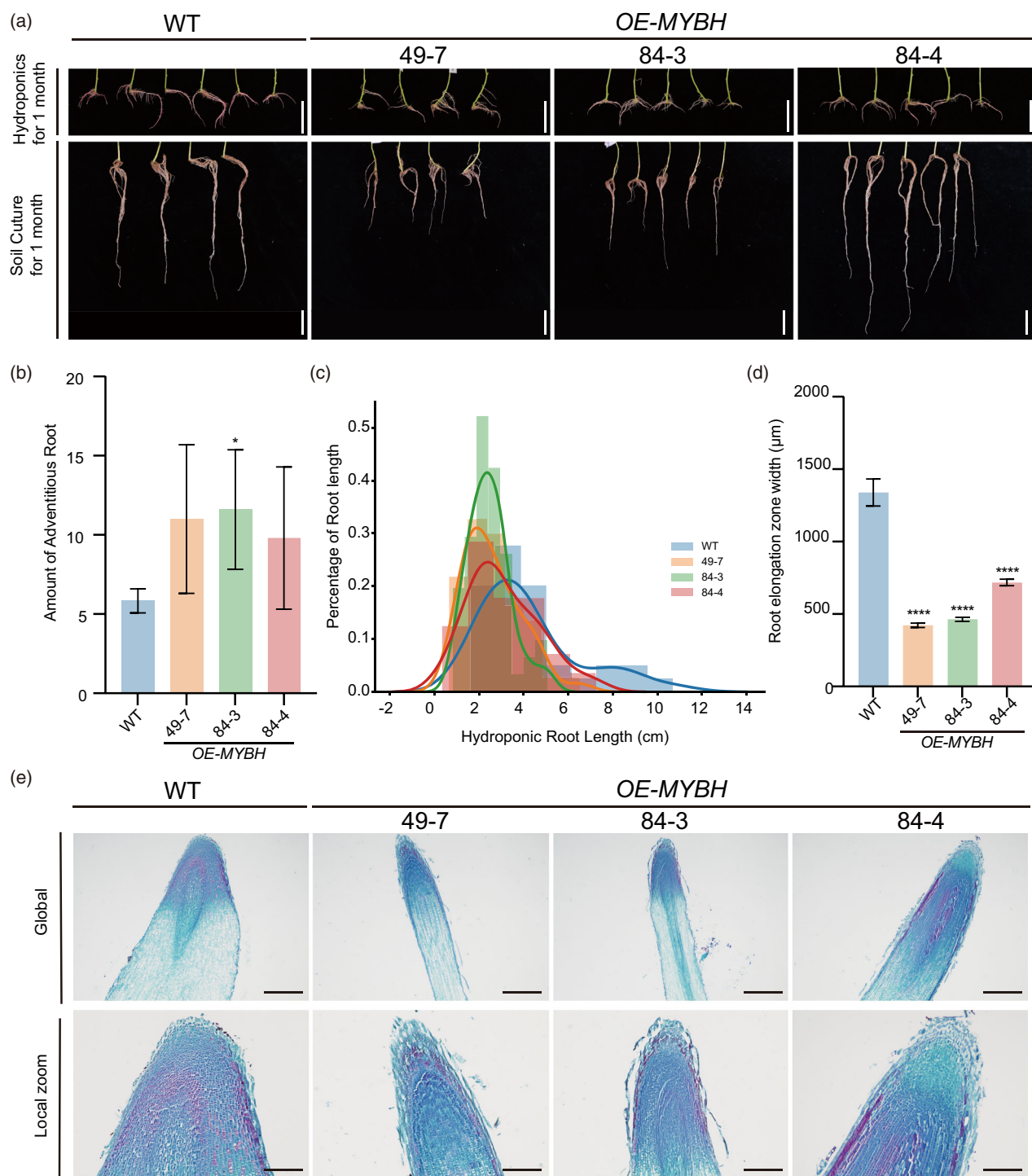
Figure 4. *PtrMYB* affects roots growth and development.

(a) Phenotype of *OE-MYBH (49–7, 84–3, 84–4)* and WT roots grown in hydroponics for 1 month and soil culture for 1 month (scale bar = 5 cm).

(b) The bar chart shows number of adventitious roots and (c) The line chart shows the percentage of root length after 1 month in hydroponics.

(d) The bar chart shows the width of elongation zone after 38 days of soil culture. Values are means ± SD, *n* = 4,5,6. *$P < 0.05$, ***$P < 0.001$, ****$P < 0.0001$. One-way ANOVA with Dunnett's test.

(e) Root tip section after 38 days of soil culture (scale bar = 500 μm) and local zoom (scale bar = 200 μm).
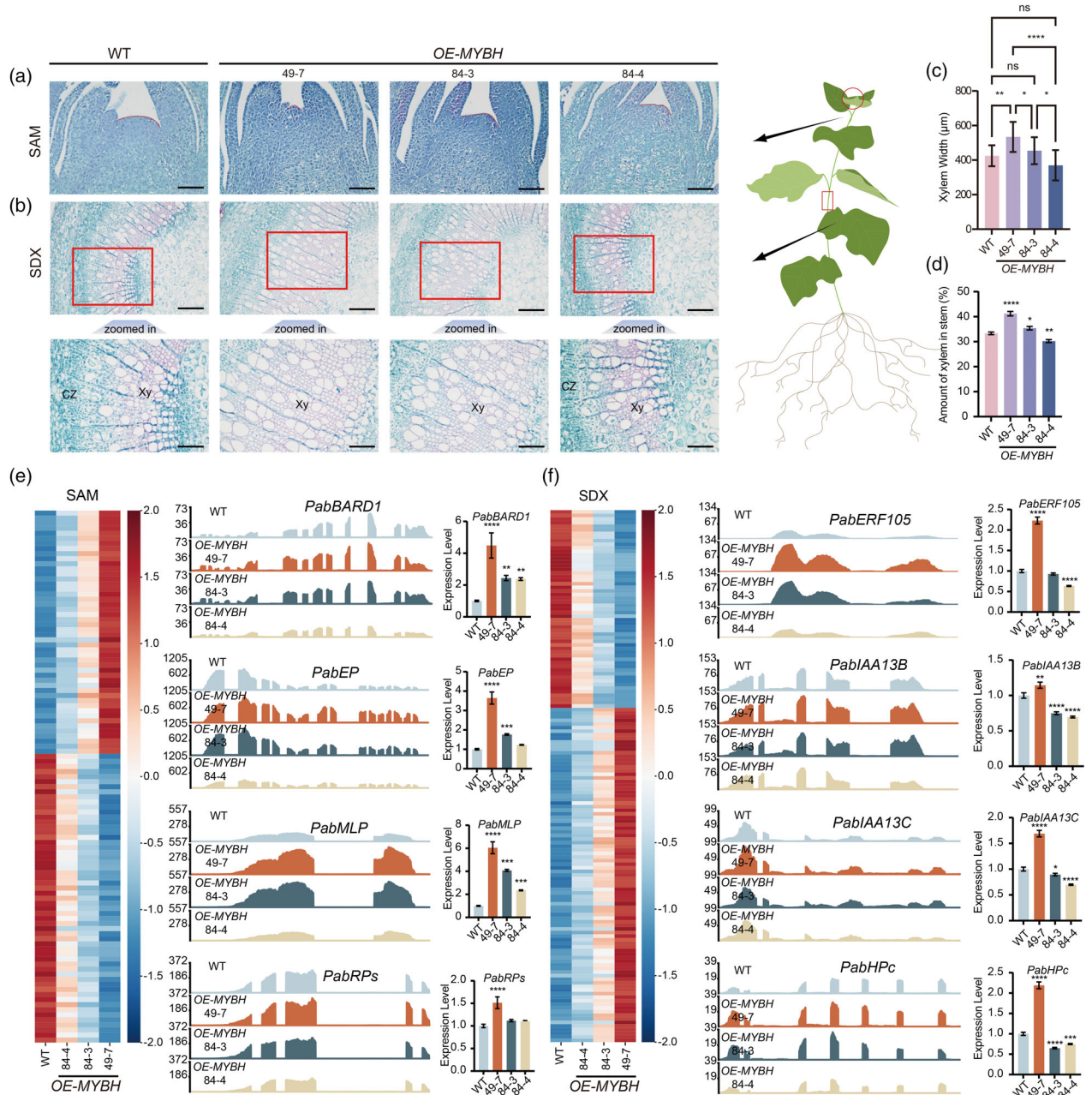
Figure 5. Cellular sections and transcriptome analysis of SAM and SDX.

(a) Cytology images of the SAM from *OE-MYBH* and WT (scale bar = 100 μm).

(b) Cytology images of SDX (scale bar = 200 μm) and its partial enlarged detail (scale bar = 100 μm). Xy, xylem; Ph, phloem; CZ, cambium zone.

(c) The bar chart shows the width of the area covered by xylem. Values are means ± SD, $n = 3$. *$P < 0.05$, **$P < 0.01$, ****$P < 0.0001$, One-way ANOVA with Dunnett's test.

(d) The bar chart shows the proportion of the xylem. The proportion of the xylem in the entire stem segment is obtained by dividing the area of the xylem by the total cross-sectional area of the stem. Values are means ± SD, $n = 6$. **$P < 0.01$.

(e) Heatmap of DEGs in the SAM from WT and *OE-MYBH*. Wiggle plot and RT-qPCR showing gene expression levels for *PabBARD1*, *PabEP*, *PabMLP*, and *PabRPs* in SAM from WT and *OE-MYBH*. Values are means ± SD, $n = 3$. *$P < 0.05$, **$P < 0.01$, ***$P < 0.001$, ****$P < 0.0001$. One-way ANOVA with Dunnett's test.

(f) Heatmap of DEGs in SDX from WT and *OE-MYBH*. Wiggle plot and RT-qPCR showing gene expression levels for *PabERF105*, *PabIAA13B*, *PabIAA13C*, and *PabHPc* in SDX from WT and *OE-MYBH*.

PtrMYBH responds to ABA treatment

Under normal growth conditions, line 84–4 exhibited minimal phenotypic differences compared with WT, likely due to insufficient *PtrMYBH* expression levels to trigger observable effects. To investigate the response of *PtrMYBH* to ABA, we treated 45-day-old WT and *OE-MYBH* (*84–4*) plants with either mock control (water) or 200 μM ABA. The treated plants exhibited obvious leaf death compared with the control group, and leaf drop occurred earlier from the lower leaves in the ABA-treated group (Figure 6a). Measurements and photographic recordings over 11 consecutive days revealed significant suppression of growth in the ABA-treated group, including reductions in ground diameter (Figure 6b) and plant height (Figure 6c), consistent with the untreated overexpression lines (49–7, 84–3, and 84–4). Additionally, *MYBH* expression was significantly higher in the ABA-treated group compared with the control group (Figure 6d). Meanwhile, in the two lines with the highest expression of *OE-MYBH* (*49–7* and *84–3*) without ABA treatment, the leaves also appeared to be curled, yellowed, and spotted with black, consistent with the phenotypes observed in the ABA-treated WT and *OE-MYBH* (*84–4*) plants (Figure 6e). Upon ABA treatment, line 84--4 recapitulated the phenotypes observed in line 49-7 (high overexpression) under normal conditions (Figure 6e). This suggests that ABA synergizes with even low levels of *PtrMYBH* (*84–4*) to amplify its regulatory effects.

DISCUSSION

Plant growth and development encompass a critical trajectory from germination to maturation, influenced by external environmental factors such as light, water, temperature, and soil, as well as the intricate interplay of genes and hormones. Genes bestow unique hereditary traits upon the plant, while hormones regulate key developmental processes through a series of complex signaling and sensing mechanisms. This includes essential milestones in plant growth, such as seed germination, leaf expansion, and flower maturation (Amasino, 2004; Santner & Estelle, 2009; Yruela, 2015). Normal ABA levels are necessary for plant development. Studies on *Arabidopsis thaliana* have demonstrated that *aba1* mutants exhibit reduced leaf size and curled margins, highlighting ABA's role in leaf organogenesis (Barrero et al., 2005). In this study, we explored the function of *PtrMYBH* in *Populus alba* "Berolinensis" and its potential involvement in an ABA-dependent pathway affecting plant growth and development. Our findings indicate that exogenous ABA application upregulates *MYBH* expression in *Populus*. MYB is known to participate in diverse aspects of plant development, metabolism, and stress response. Previous research has reported that KUA1 regulates leaf cell expansion and organ size by modulating ROS homeostasis (Lu et al., 2014). PtoMYB10 promotes SCW thickening and enhances wood fiber development (Jiang et al., 2022). Additionally, TaMpc1-D4 has been shown to inhibit root growth under drought conditions in *Arabidopsis* and wheat (Li et al., 2020) and MYB3R4 is a key TF regulating the growth and development of SAM tissue in *Arabidopsis* (Yang, Guo, et al., 2021). However, their roles in poplar remain largely uncharacterized.

Our research demonstrates that *PtrMYBH* is integral to the growth and development of *Populus*. Different levels of *PtrMYBH* overexpression resulted in phenotypic alteration, including stunted growth, dwarfism, leaf curling, deformity, localized necrosis, as well as variations in leaf size, root length, and xylem proportion. These phenotypic changes suggest that *PtrMYBH* may serve a versatile regulatory role in poplar growth. Our results indicate that exogenous ABA treatment induces *MYBH* expression, and the growth inhibition observed in plants with high *PtrMYBH* overexpression is consistent with the known effects of ABA on plant growth (Anfang & Shani, 2021). This suggests that *PtrMYBH* could be a crucial component of the ABA signaling network, highlighting its significance for plant development. Moreover, our study revealed that *PtrMYBH* affects multiple developmental aspects in poplar, including stomatal development and adventitious root growth. Alterations in stomatal morphology and density in *PtrMYBH*-overexpression lines may affect water use efficiency and transpiration rate. The elongation zone of the root tip, located between the root crown and the maturation zone, is the most active growth region. Any inhibition of root growth could consequently impair the plant's overall growth and survival.

Figure 6. Phenotypic Characteristics of Poplar Under ABA Treatment and *PtrMYBH* Response.
(a) Images of WT and *OE-MYBH* (*84–4*) under water (control) or 200 μM ABA treatment for 11 days (scale bar = 10 cm), along with localized enlargements of the apices and the 7th leaves of WT and *OE-MYBH* (*84–4*) on the 11th day of ABA treatment (scale bar = 5 cm).
(b) Changes in ground diameter in the control and the experimental groups.
(c) Changes in plant height in the control and experimental groups.
(d) *MYBH*-overexpression level in the control and experimental groups on the 11th day. Values are means ± SD, $n = 3$. *$P < 0.05$、**$P < 0.01$, ****$P < 0.0001$. One-way ANOVA with Dunnett's test. The *MYBH* sequences of *P. trichocarpa* and *P. alba* "Berolinensis" are highly similar and indistinguishable, so this expression includes both endogenous *PabMYBH* and exogenously transformed *PtrMYBH*.
(e) Photographs of plants and leaves of the control and experimental groups (the ABA-treated group) on the 11th day (scale bar = 5 cm).
(f) Schematic model of *PtrMYBH* responses ABA stress and regulates development of *Populus*.

(a)

(b)

(c)

(d)

(e)

(f)
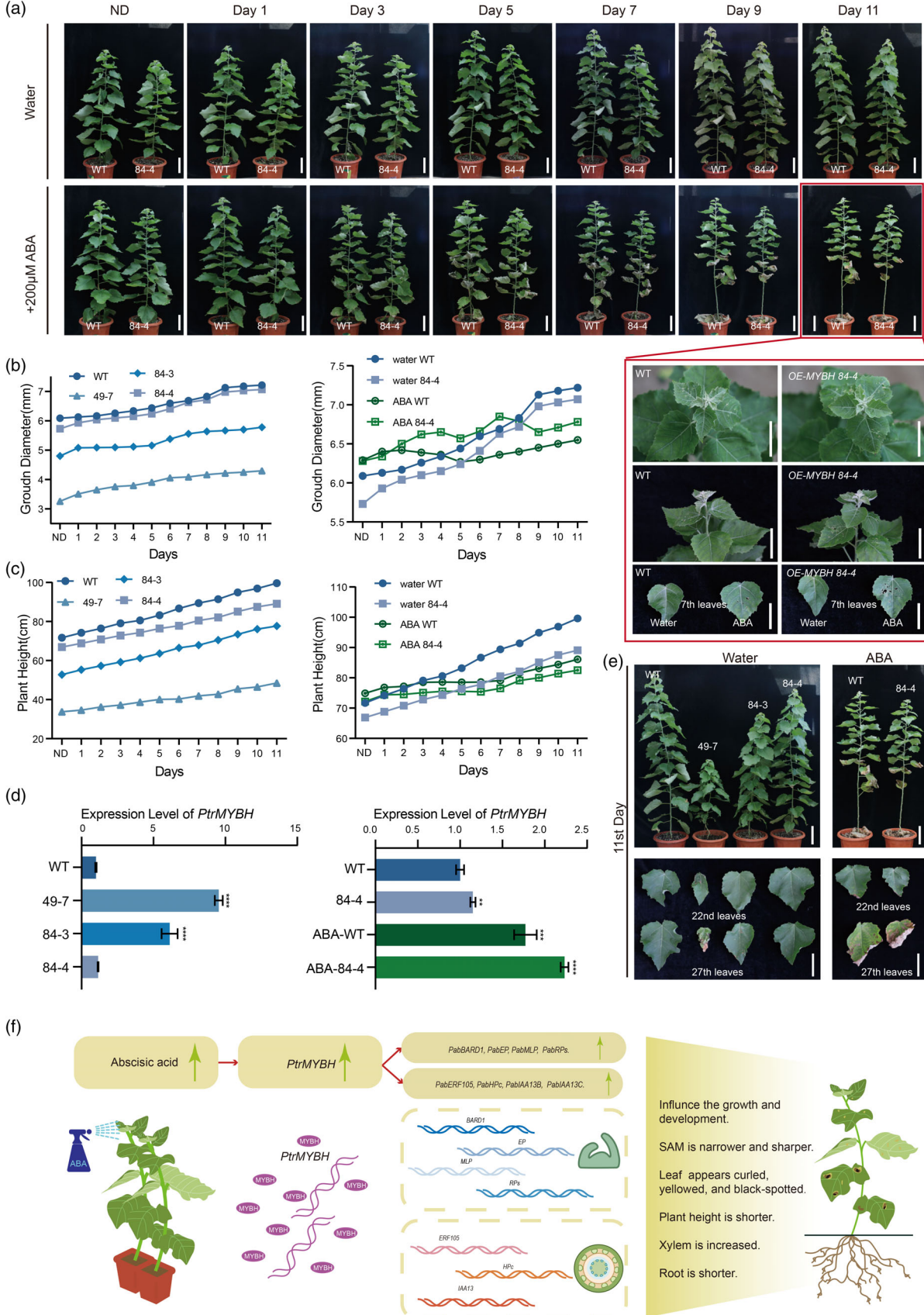
GO enrichment analysis of DEGs in *PtrMYBH*-overexpressing poplars points to its involvement in regulating the cell cycle, stress response, and metabolic processes. This is consistent with the known diverse roles of MYB in plants, including cell growth, differentiation, and environmental stress responses. To identify enriched motifs, we extracted the 2 kb upstream promoter regions of DEGs using all gene promoters as background, with the default parameters in HOMER software. Our analysis revealed the enriched motifs of DEGs in SAM (GGTAGGTR) and SDX (TTACCTAACT), respectively. However, the above enriched motifs represent potential regulatory elements associated with the DEGs. These motifs may not directly correspond to MYBH binding motifs. To more comprehensively investigate binding motifs, further studies using genome-wide methods like chromatin immunoprecipitation (ChIP) assay are necessary to elucidate the precise binding sites of *PtrMYBH* and explore its broader implications for poplar cultivation and improvement.

To strengthen our findings, we have conducted additional experiments using RNAi-mediated transient silencing of *PabMYBH* in protoplasts from xylem of *P. alba "Berolinensis"*. The RNAi vector effectively reduced *PabMYBH* expression levels by 40% in *RNAi-MYBH* compared with WT (Figure S8A). The RNAi-*PabMYBH* line exhibited a 40% reduction in *PabMYBH* expression compared with WT based on qPCR result (Figure S8B). We detect differential expression of *PabBARD1*, *PabEP*, *PabMLP*, *PabEFR105*, *PabIAA13C*, and *PabHPc* in the *RNAi-MYBH* lines compared with the WT (Figure S8C). Among the four upregulated genes in three MYBH-overexpression line (*49–7, 84–3*, and *84–4*), *PabEP* and *PabRPs* showed opposite regulation (upregulated in OE but downregulated in RNAi), suggesting they are likely direct targets of MYBH. In contrast, *PabBARD1* and *PabMLP* were consistently upregulated in both systems, implying indirect regulation. Future studies using ChIP-seq and yeast one-hybrid assays will help definitively identify direct targets. Our combined overexpression and RNAi-silencing data support the role of *PtrMYBH* in modulating gene expression. However, it is not possible to observe the phenotypic changes by protoplast RNAi. Thus, more rigorous conclusion could be drawn in future studies by obtaining stable gene-edited or RNAi transgenic materials to observe phenotypic changes and compare them with overexpression phenotypes.

CONCLUSIONS

In summary, our study revealed the complex role of *PtrMYBH* in the growth and development of poplar and its potential integration with the ABA signaling pathway. Future studies are needed to elucidate the exact molecular mechanisms of *PtrMYBH* functions and to understand its broader implications for poplar cultivation and improvement under varying environmental conditions.

MATERIALS AND METHODS

Plant materials and ABA treatment

Populus alba "Berolinensis" (*P. alba "Berolinensis"*) and *P. trichocarpa* were grown in a greenhouse with an average temperature of 22°C, and a 16-h light/8-h dark cycle. The soil mixture consisted of natural soil and peat moss (PINDSTRUP PLUS) in a 2:1 dry weight ratio. Plants were watered every 2 days and fertilized monthly with a 20-20-20 N/P/K compound fertilizer. Sterile *P. alba "Berolinensis"* plants were propagated on 1/2 MS media (Phytotech, no. M519, America) (pH 5.8) supplemented with 30 g/L sucrose, 8 g/L agar, and 0.1 mg/L α-naphthaleneacetic acid (NAA, storage concentration of 1 mg/mL NAA). To assess the role of *MYBH* under ABA treatment, 45-day-old *P. alba "Berolinensis"* plants in the greenhouse were sprayed with a 200 μM ABA solution (LABLEAD, no. ABA01, China), applied to both leaf surfaces daily for 11 days.

Construction of transcriptome libraries and bioinformatics analysis of ABA-treated *Populus trichocarpa*

For ABA-treated transcriptome experiments, 6-month-old clonally propagated *P. trichocarpa* in 15-cm pots (one plant per pot) uniform size and vigor were used for ABA treatment with 100-μM solution. *P. trichocarpa* plants were divided into three groups: (1) control (0-h ABA treatment), (2) 24-h ABA treatment, and (3) 48-h ABA treatment. All plants were well-watered before ABA treatment. Material collection included: (a) stem-differentiating xylem (SDX) and phloem scrapped from the stem below the seventh leaves after debarking, (b) tender shoot tip above the second node, (c) leaves with main veins removed from the fifth node (Figure 1a). All biological samples were wrapped with tinfoil, frozen in liquid nitrogen immediately, and stored at −80°C (Shen et al., 2019). Total RNAs were isolated from SDX, phloem, young shoot tip, and leaves of 6-month-old *P. trichocarpa* using an RNAprep Pure Plant Kit (Polysaccharides & Polyphenolics-rich) (Tiangen, no. DP441, China), followed by DNase I to remove DNA. RNA quality and concentration were assessed using a NanoDrop 2000 spectrophotometer (Thermo scientific). The RNA samples were subsequently used for RNA-seq and Reverse Transcription Quantitative Polymerase Chain Reaction (RT-qPCR). For RT-PCR, 1 μg of total RNA from each sample was reverse transcribed into cDNA using First-Strand cDNA Synthesis SuperMix (gDNA digester plus) (YEASEN, no. 11141ES10, Shanghai, China). RT-qPCR was performed using Hieff qPCR SYBR Green Master Mix (YEASEN, no. 11202ES08, Shanghai, China) on an Agilent M × 3005P RealTime PCR System, following the manufacturer's instructions, with *EF1α* as the internal control. Gene expression was quantitatively assessed using the comparative $2^{-\Delta\Delta Ct}$ method. All RT-qPCR primers are provided in Table S1.

For RNA-seq, tissues from xylem, phloem, shoot tip, and leaves at 0, 24, and 48 h under ABA treatment were collected to created rRNA-depleted RNA-seq libraries using dUTP method. High-quality reads were generated using ht2-filter (version 1.92.1) from HTQC package (Yang et al., 2013) with default option. All mapped reads were counted by hisat2 2.1.0 (Kim et al., 2019) using annotated genes and sequences from the *P. trichocarpa* genome (V3.55). DEGs were identified using the DESeq2 (Wald test), with an absolute log2FC (fold change) >2 and FDR <0.05. All genes with gene ontology (GO) were annotated using eggNOG-mapper (v2.1.12) with default parameters. GO enrichment analysis was conducted with clusterProfiler (Wu et al., 2021), mapping these DEGs to their respective GO terms and calculating enrichment *P*-values for each term using hypergeometric tests.

Ultimately, GO terms with *P*-values less than 0.05 were considered as significantly enriched terms.

Generation of transgenic PtrMYBH *P. Alba "Berolinensis"*

The plant expression vector pBI121 was double-digested with *BamHI* and *SacI*, followed by agarose gel electrophoresis; the desired linearized enzyme-cut product is cut and subjected to gel purification. Full-length cDNAs encoding *PtrMYBH* were amplified by using $2\times$ Phanta Flash Master Mix (Dye Plus) (Vazyme, no. P520-01, Nanjing, China) and inserted downstream of the 35S promoter in the pBI121 vector using ClonExpress Ultra One Step Cloning Kit (Vazyme, no. C115-01, China, Nanjing, China) to produce the 35S:*PtrMYBH-3 × flag* constructs. The vector constructs were introduced into Trelief™ 5α Chemically Competent Cell (TSINGKE, no. TSC-C01, China) of *Escherichia coli*.

After confirming the correctness of the constructs by DNA sequencing, the plasmids were introduced into *Agrobacterium tumefaciens* for transformation of *P. alba "Berolinensis"* by leaf-disk transformation (Wang et al., 2011). Pre-activated *Agrobacterium* containing the vector was picked and transferred to MS infection solution supplemented with acetosyringone (AS). The solution was mixed until uniform, and the OD_{600} of the bacterial suspension was adjusted to 0.6–0.8, followed by incubation for 20 min. Fully expanded leaves from 1.5-month-old plantlets were cut into 1 cm^2 leaf disks and incubated with the suspended *Agrobacterium* for 15–20 min. The leaf discs were blotted with sterile filter paper to remove the excess bacteria and then quickly laid flat dorsal side down in MS co-culture medium with AS and incubated in the dark for 3 days. The co-cultivated leaves were transferred to MS medium (MS, 0.1 mg/L NAA, 0.2 mg/L 6-BA, 0.01 mg/L TDZ, 30 g/L sucrose, 3.5 g/L Phytagel, pH 5.8) with 200 mg/L Timentin (Tim) and 50 mg/L Kanamycin every 10 day for shoot induction. Once resistant buds appeared, they were transferred to selective medium (1/2 MS, 30 g/L sucrose, 0.1 mg/L NAA, 8 g/L agar, 200 mg/L Tim, pH 5.8). RT-qPCR were used to identify transgenic plants.

Observation of leaf phenotyping in MYBH transgenic *P. Alba "Berolinensis"*

The fourth fully extended leaf from 45-days-old transgenic lines, grown on 1/2 MS media (pH 5.8), was chosen for further phenotypic analysis. To measure stomatal features, samples were obtained by punching holes, avoiding leaf veins. These samples were then immersed in fixative [3:1(v/v) mix of anhydrous ethanol: acetic acid] for 24 h and washed three times with deionized water (ddH_2O). The samples were turned into clearing solution [8:2:1 (w/v/v) mix of chloral hydrate l: H_2O: glycerol] overnight. Images were captured using a Zeiss Axio Imager A1 microscopy (Carl Zeiss, Oberkochen, Germany).

RNA sequencing of MYBH transgenic *P. Alba "Berolinensis"* and bioinformatics analysis

Total RNA was extracted from SDX and shoot tips of 2-month-old *MYBH*-overexpressing lines (*49-7, 84-3,* and *84-4*) and WT using an RNAprep Pure Kit (polysaccharides and polyphenolics-rich) (Tiangen; no. DP441) following the manufacturer's instructions. RNA library preparation and sequencing were performed based on dUTP methods with poly(A) selection. The *P. alba "Berolinensis"* genome (Chen et al., 2023) was used for transcriptome alignment. All other transcriptomic analyses followed the same analytical pipeline as applied to the ABA-treated transcriptome data.

Histochemical staining and microscopic analysis of MYBH-overexpressing lines

Shoot apical meristems (SAM), roots, stems, and leaves from *MYBH*-overexpressing *P. alba "Berolinensis"* were harvested and immersed overnight in (70%, 50%) formaldehyde–acetic acid–ethanol fixative (FAA) solution (Servicebio, Wuhan, China). The samples were gradually dehydrated by immersing them in a series of increasing ethanol concentrations (30%, 40%, 50%, 60%, 70%, 85%, and 95%). Transfer the dehydrated samples to different ratios of ethanol/xylene solutions (1:0, 3:1, 1:1, 1:3, 0:1) for transparency. After embedding, sectioning, the samples were stained with Safranin O-Fast Green Staining. Cross-sections of all samples were observed, and images were captured using a Nikon Ni-U DIC upright microscope (Nikon, Tokyo, Japan).

Statistical analyses

For comparisons between two groups, we used unpaired two-tailed Student's t-test. For comparisons among multiple groups (e.g., WT control versus three overexpression lines), we performed one-way analysis of variance (ANOVA), followed by Dunnett's test for multiple comparisons. Analyses were performed using GraphPad Prism 9.0 for Windows (GraphPad Software, La Jolla, CA, United States). Significance was determined at *P*-value <0.05.

Histochemical detection of reactive oxygen species

Leaf samples (3rd, 5th, and 7th positions) from 1.5-month-old *P. alba* "*Berolinensis*" plants were harvested for analysis. H_2O_2 was detected using 3,3′-diaminobenzidine (DAB, 1 mg/mL, pH 3.8) for 2.5 h under dark conditions, which undergoes peroxidase catalysis in the presence of H_2O_2 to form brown precipitates. We also detected H_2O_2 concentrations using a commercial Hydrogen Peroxide Content Assay Kit (Microscale method) following the manufacturer's protocol (HRbio, no. HRK0520, China). Superoxide anions (O_2^-) were visualized through nitroblue tetrazolium (NBT, 0.5 mg/mL, pH 6.0) solution for 2.5 h under dark conditions. Following staining, samples were destained in 95% ethanol until complete chlorophyll extraction.

RNAi vector construction and validation

A 203 bp conserved domain of *PabMYBH* was selected for RNAi vector construction. Both sense and antisense shRNA were amplified using $2\times$ Phanta Flash Master Mix (Vazyme, no. P520-01, Nanjing, China) with CaMV 35S promoter and NOS terminator. Transformation efficiency in *P. alba "Berolinensis"* xylem protoplasts was evaluated using pUC22-EGFP. The recombinant vector was constructed through a two-step cloning procedure. First, the pUC22 vector was double-digested with *HindIII* and *NcoI* restriction enzymes, followed by the insertion of the CaMV 35S promoter and *RNAi-PabMYBH sense* fragment to generate the primary construct using ClonExpress Ultra One Step Cloning Kit (Vazyme, no. C115-01, China, Nanjing, China). Subsequently, the secondary structure was engineered by utilizing a partial fragment of the primary vector as the loop region. This intermediate vector was subjected to *MfeI* single digestion, enabling precise integration of the *RNAi-PabMYBH antisense* fragment and NOS terminator through seamless cloning. This resulted in a complete RNA interference (RNAi) expression cassette containing both sense and antisense of *PabMYBH* flanking the loop structure, under the transcriptional control of the constitutive 35S promoter with NOS termination signals. Final constructs were transformed into Trelief™ 5α Chemically *E. coli* Cell (TSINGKE, no. TSC-C01, China).

Protoplast isolation and transfection

Stems from two-month-old *P. alba "Berolinensis"* were peeled to remove the outer layer, cut into 10 cm segments, and immersed in 40 mL freshly prepared enzymolysis solution [0.2 M MES (pH 5.7) 4 mL, 0.8 M D-mannitol 25 mL, 2 M KCl 0.4 mL, 1 M CaCl$_2$ 0.4 mL, 10% BSA 0.4 mL, Cellulase R-10 0.6 g, Macerozyme R-10 0.16 g, adjusted to 40 mL with ddH$_2$O] for 3 h in dark. After enzymatic digestion, stem segments were immersed in 30 mL MMG solution [0.8 M D-mannitol 15.625 mL, 0.2 M MES (pH 5.7) 1 mL, 1 M MgCl$_2$ 0.75 mL, adjusted to 50 mL with ddH$_2$O] under gentle orbital shaking. The protoplast suspension was filtered through 70 μm nylon mesh (two layers), and centrifuged (500g, 3 min). After supernatant removal, protoplasts were resuspended in MMG solution to achieve a final protoplast concentration of 2×10^5 cells/mL.

For transfection, 10 μL plasmid DNA (2000 ng/μL) was mixed with 100 μL protoplasts and 110 μL PEG4000 solution [0.8 M D-mannitol 0.25 mL, 1 M CaCl$_2$ 0.1 mL, PEG4000 0.4 g, adjusted to 1 mL with ddH$_2$O]. After incubation at 25°C for 10 min, 440 μL WI solution [0.2 M MES (pH 5.7) 1 mL, 0.8 M D-mannitol 15.625 mL, 2 M KCl 0.5 mL, adjusted to a final volume of 50 mL with ddH$_2$O] was added, followed by centrifugation at 500 g for 3 min and discarding the supernatant. The protoplasts were resuspended in 1 mL WI solution and transferred into 2 mL centrifuge tubes pre-coated with 1% (w/v) bovine serum albumin (BSA), then incubated in darkness at 25°C for 12 h. Subsequently, transformation efficiency was quantified through fluorescence microscopy.

AUTHOR CONTRIBUTIONS

LG conceived and designed the study. ZL, XF, XL, YY, SX, XZ, TL, SL, and DY performed the experiments. ZZ, XL, TH, MZ, and HZ analyzed the high-throughput sequencing data. ZL, XF, XL, and LG wrote the manuscript. All authors have read and approved the final version.

ACKNOWLEDGEMENTS

CONFLICT OF INTEREST

The authors declare that they have no competing interests.

DATA AVAILABILITY STATEMENT

The Illumina RNA-seq raw data from this study are available in NGDC (https://ngdc.cncb.ac.cn/) under accession numbers CRA019430 (for ABA-treated SDX, phloem, shoot tip, and leaves at 0, 24, and 48 h) and CRA019548 (for WT and *OE-MYBH*, including *49–7*, *84–3*, and *84–4*).

SUPPORTING INFORMATION

Additional Supporting Information may be found in the online version of this article.

Figure S1. Bubble plot displaying tissue-enriched GO terms, with panels A–D representing leaf, xylem, shoot tip, and phloem tissues respectively.

Figure S2. Bubble plot illustrating GO term enrichment analysis of five major gene clusters identified from ABA-responsive genes in leaf tissue.

Figure S3. Bubble plot illustrating GO term enrichment analysis of five major gene clusters identified from ABA-responsive genes in shoot tip tissue.

Figure S4. Bubble plot illustrating GO term enrichment analysis of five major gene clusters identified from ABA-responsive genes in xylem tissue.

Figure S5. Bubble plot illustrating GO term enrichment analysis of five major gene clusters identified from ABA-responsive genes in phloem tissue.

Figure S6. ABA-responsive TFs and *PtrMYBH* expression dynamics. (A) Classification and number of ABA response TF across four tissue types (leaf, shoot tip, phloem, and xylem). (B) *PtrMYBH* expression dynamics under ABA treatment. Line plot shows transcript levels in four tissues; *P*-values indicate significance (Wald test, DESeq2) of ABA 48 h versus 0 h comparisons.

Figure S7. Detection of H$_2$O$_2$ concentration and expression of peroxidase genes. (A) H$_2$O$_2$ concentration. Values are means ± SD, $n = 3$. *$P < 0.05$, ****$P < 0.0001$, One-way ANOVA with Dunnett's test. (B) Bar graph presented expression of peroxidase genes (). (C) Wiggle plots presented transcriptomic profiles of two genes.

Figure S8. Molecular analysis of RNAi-mediated *PabMYBH* silencing. (A) Schematic diagram of *PabMYBH* CDS. (B) Schematic diagram of the RNAi-*PabMYBH* vector structure. (C) Expression level of *PabMYBH*. Values are means ± SD, $n = 3$. ***$P < 0.001$, Student's *t*-test. (D) Effects of *PabMYBH*-RNAi on the expression of related genes: *PabBARD1*, *PabEP*, *PabMLP*, *PabRPs*, *PabERF105*, *PabIAA13B*, *PabIAA13C*, and *PabHPc* from WT and *RNAi-MYBH*. Values are means ± SD, $n = 3$. **$P < 0.01$, ***$P < 0.001$, Student's *t*-test.

Table S1. The primer set used in this study are provided.

Table S2. Expression matrix of four tissues (leaf, shoot tip, phloem, xylem) across ABA treatment timepoints (0, 24, 48 h) in *Populus trichocarpa*.

Table S3. DEGs analysis under ABA treatment, including fold change, and *P*-values.

Table S4. Tissue-specific highly expressed gene lists (leaf, shoot tip, phloem, xylem).

Table S5. GO enrichment analysis of tissue-specific highly expressed genes.

Table S6. Expression profiles of ABA-responsive clustered genes in leaf tissue.

Table S7. Expression profiles of ABA-responsive clustered genes in shoot tip tissue.

Table S8. Expression profiles of ABA-responsive clustered genes in xylem tissue.

Table S9. Expression profiles of ABA-responsive clustered genes in phloem tissue.

Table S10. GO enrichment analysis of ABA-responsive gene clusters in leaf tissue.

Table S11. GO enrichment analysis of ABA-responsive gene clusters in shoot tip tissue.

Table S12. GO enrichment analysis of ABA-responsive gene clusters in xylem tissue.

Table S13. GO enrichment analysis of ABA-responsive gene clusters in phloem tissue.

Table S14. The list of ABA-responsive TFs.

Table S15. Expression matrix of in SDX and SAM from WT and *PtrMYBH*-overexpressing *P. alba "Berolinensis."*

REFERENCES

Ali, F., **Qanmber, G.**, **Li, F.** & **Wang, Z.** (2022) Updated role of ABA in seed maturation, dormancy, and germination. *Journal of Advanced Research*, **35**, 199–214.

Amasino, R. (2004) Vernalization, competence, and the epigenetic memory of winter. *The Plant Cell*, **16**, 2553–2559.

Anfang, M. & **Shani, E.** (2021) Transport mechanisms of plant hormones. *Current Opinion in Plant Biology*, **63**, 102055.

Barrero, J., **Piqueras, P.**, **González-Guzmán, M.**, **Serrano, R.**, **Rodríguez, P.**, **Ponce, M.** *et al.* (2005) A mutational analysis of the ABA1 gene of *Arabidopsis thaliana* highlights the involvement of ABA in vegetative development. *Journal of Experimental Botany*, **56**, 2071–2083.

Chen, Y., **Zhang, X.**, **Wu, W.**, **Chen, X.**, **Gu, H.**, **Qu, L.** (2006) Overexpression of the Wounding-Responsive Gene AtMYB15 Activates the Shikimate Pathway in Arabidopsis. *J Integr Plant Biol*, **48**, 1084–1095.

Chen, K., **Li, G.**, **Bressan, R.**, **Song, C.**, **Zhu, J.** & **Zhao, Y.** (2020) Abscisic acid dynamics, signaling, and functions in plants. *Journal of Integrative Plant Biology*, **62**, 25–54.

Chen, S., **Yu, Y.**, **Wang, X.**, **Wang, S.**, **Zhang, T.**, **Zhou, Y.** *et al.* (2023) Chromosome-level genome assembly of a triploid poplar *Populus alba* 'Berolinensis'. *Molecular Ecology Resources*, **23**, 1092–1107.

Cramer, G. & **Quarrie, S.** (2002) Abscisic acid is correlated with the leaf growth inhibition of four genotypes of maize differing in their response to salinity. *Functional Plant Biology*, **29**, 111–115.

Cutler, S., **Rodriguez, P.**, **Finkelstein, R.** & **Abrams, S.** (2010) Abscisic acid: emergence of a core signaling network. *Annual Review of Plant Biology*, **61**, 651–679.

Dubos, C., **Stracke, R.**, **Grotewold, E.**, **Weisshaar, B.**, **Martin, C.** & **Lepiniec, L.** (2010) MYB transcription factors in Arabidopsis. *Trends in Plant Science*, **15**, 573–581.

Humplík, J., **Bergougnoux, V.** & **Volkenburgh, E.** (2017) To stimulate or inhibit? That is the question for the function of abscisic acid. *Trends in Plant Science*, **22**, 830–841.

Jiang, P., **Lin, X.**, **Bian, X.**, **Zeng, Q.** & **Liu, Y.** (2022) Ectopic expression of Populus MYB10 promotes secondary cell wall thickening and inhibits anthocyanin accumulation. *Plant Physiology and Biochemistry*, **172**, 24–32.

Jiao, B., **Zhao, X.**, **Lu, W.**, **Guo, L.** & **Luo, K.** (2019) The R2R3 MYB transcription factor MYB189 negatively regulates secondary cell wall biosynthesis in Populus. *Tree Physiology*, **39**, 1187–1200.

Kim, D., **Paggi, J.**, **Park, C.**, **Bennett, C.** & **Salzberg, S.** (2019) Graph-based genome alignment and genotyping with HISAT2 and HISAT-genotype. *Nature Biotechnology*, **37**, 907–915.

Ko, J., **Prassinos, C.**, **Keathley, D.** & **Han, K.** (2011) Novel aspects of transcriptional regulation in the winter survival and maintenance mechanism of poplar. *Tree Physiology*, **31**, 208–225.

Leung, J. & **Giraudat, J.** (1998) Abscisic acid signal transduction. *Annual Review of Plant Biology*, **49**, 199–222.

Li, X., **Tang, Y.**, **Li, H.**, **Luo, W.**, **Zhou, C.**, **Zhang, L.** *et al.* (2020) A wheat R2R3 MYB gene TaMpc1-D4 negatively regulates drought tolerance in transgenic Arabidopsis and wheat. *Plant Science*, **299**, 110613.

Liu, J., **Osbourn, A.** & **Ma, P.** (2015) MYB transcription factors as regulators of phenylpropanoid metabolism in plants. *Molecular Plant*, **8**, 689–708.

Long, T., **Yang, F.**, **Chen, Z.**, **Xing, Y.**, **Tang, X.**, **Chen, B.** *et al.* (2024) Overexpression of PtoMYB99 diminishes poplar tolerance to osmotic stress by suppressing ABA and JA biosynthesis. *Journal of Plant Physiology*, **292**, 154149.

Lu, D., **Wang, T.**, **Persson, S.**, **Mueller-Roeber, B.** & **Schippers, J.** (2014) Transcriptional control of ROS homeostasis by KUODA1 regulates cell expansion during leaf development. *Nature Communications*, **5**, 3767.

Luo, X., **Chen, Z.**, **Gao, J.** & **Gong, Z.** (2014) Abscisic acid inhibits root growth in Arabidopsis through ethylene biosynthesis. *The Plant Journal*, **79**, 44–55.

Miao, C., **Xiao, L.**, **Hua, K.**, **Zou, C.**, **Zhao, Y.**, **Bressan, R.A.** *et al.* (2018) Mutations in a subfamily of abscisic acid receptor genes promote rice growth and productivity. *Proceedings of the National Academy of Sciences of the United States of America*, **115**, 6058–6063.

Ortiz-García, P., **Pérez-Alonso, M.M.**, **González Ortega-Villaizán, A.**, **Sánchez-Parra, B.**, **Ludwig-Müller, J.**, **Wilkinson, M.D.** *et al.* (2022) The Indole-3-acetamide-induced Arabidopsis transcription factor MYB74

decreases plant growth and contributes to the control of osmotic stress responses. *Frontiers in Plant Science*, **13**, 928386.

Plett, J., **Wilkins, O.**, **Campbell, M.**, **Ralph, S.** & **Regan, S.** (2010) Endogenous overexpression of Populus MYB186 increases trichome density, improves insect pest resistance, and impacts plant growth. *The Plant Journal*, **64**, 419–432.

Raghavendra, A.S., **Gonugunta, V.**, **Christmann, A.** & **Grill, E.** (2010) ABA perception and signalling. *Trends in Plant Science*, **15**, 395–401.

Reyes, J. & **Chua, N.** (2007) ABA induction of miR159 controls transcript levels of two MYB factors during Arabidopsis seed germination. *Plant Journal*, **49**, 592–606.

Santner, A. & **Estelle, M.** (2009) Recent advances and emerging trends in plant hormone signalling. *Nature*, **459**, 1071–1078.

Shen, L., **Liang, Z.**, **Wong, C.** & **Yu, H.** (2019) Messenger RNA modifications in plants. *Trends in Plant Science*, **24**, 328–341.

Shi, M., **Liu, X.**, **Zhang, H.**, **He, Z.**, **Yang, H.**, **Chen, J.** *et al.* (2020) The IAA- and ABA-responsive transcription factor CgMYB58 upregulates lignin biosynthesis and triggers juice sac granulation in pummelo. *Horticulture Research*, **7**, 139.

Stolarski, M.J., **Gil, Ł.**, **Krzyżaniak, M.**, **Olba-Zięty, E.** & **Wu, A.** (2024) Willow, poplar, and black locust debarked wood as feedstock for energy and other purposes. *Energies*, **17**, 1535.

Sun, L.R., **Wang, Y.B.**, **He, S.B.** & **Hao, F.S.** (2018) Mechanisms for abscisic acid inhibition of primary root growth. *Plant Signaling & Behavior*, **13**, e1500069.

Sun, W., **Ma, Z.**, **Chen, H.** & **Liu, M.** (2019) MYB gene family in potato (Solanum tuberosum L.): genome-wide identification of hormone-responsive reveals their potential functions in growth and development. *International Journal of Molecular Sciences*, **20**, 4847.

Tang, F., **Jiao, B.**, **Zhang, M.**, **He, M.**, **Su, R.**, **Luo, K.** *et al.* (2023) PtoMYB031, the R2R3 MYB transcription factor involved in secondary cell wall biosynthesis in poplar. *Frontiers in Plant Science*, **14**, 1341245.

Wang, H., **Wang, H.**, **Liu, H.**, **Tang, R.** & **Zhang, H.** (2011) An efficient agrobacterium-mediated transformation and regeneration system for leaf explants of two elite aspen hybrid clones Populus alba× P. Berolinensis and Populus davidiana× P. Bolleana. *Plant Cell Reports*, **30**, 2037–2044.

Wu, T., **Hu, E.**, **Xu, S.**, **Chen, M.**, **Guo, P.**, **Dai, Z.** *et al.* (2021) clusterProfiler 4.0: a universal enrichment tool for interpreting omics data. *The Innovation*, **2**, 100141.

Xu, C., **Shen, Y.**, **He, F.**, **Fu, X.**, **Yu, H.**, **Lu, W.** *et al.* (2019) Auxin-mediated aux/IAA-ARF-HB signaling cascade regulates secondary xylem development in Populus. *New Phytologist*, **222**, 752–767.

Yang, W., **Cortijo, S.**, **Korsbo, N.**, **Roszak, P.**, **Schiessl, K.**, **Gurzadyan, A.** *et al.* (2021) Molecular mechanism of cytokinin-activated cell division in Arabidopsis. *Science*, **371**, 1350–1355.

Yang, X., **Guo, T.**, **Li, J.**, **Chen, Z.**, **Guo, B.** & **An, X.** (2021) Genome-wide analysis of the MYB-related transcription factor family and associated responses to abiotic stressors in Populus. *International Journal of Biological Macromolecules*, **191**, 359–376.

Yang, X., **Liu, D.**, **Liu, F.**, **Wu, J.**, **Zou, J.**, **Xiao, X.** *et al.* (2013) HTQC: a fast quality control toolkit for Illumina sequencing data. *BMC Bioinformatics*, **14**, 33.

Yoshida, T., **Christmann, A.**, **Yamaguchi-Shinozaki, K.**, **Grill, E.** & **Fernie, A.** (2019) Revisiting the basal role of ABA - roles outside of stress. *Trends in Plant Science*, **24**, 625–635.

Yruela, I. (2015) Plant development regulation: overview and perspectives. *Journal of Plant Physiology*, **182**, 62–78.

Zhai, K., **Zhao, G.**, **Jiang, H.**, **Sun, C.** & **Ren, J.** (2020) Overexpression of maize ZmMYB59 gene plays a negative regulatory role in seed germination in Nicotiana tabacum and Oryza sativa. *Frontiers in Plant Science*, **11**, 564665.

Zhang, L., **Xu, Y.**, **Li, Y.**, **Zheng, S.**, **Zhao, Z.**, **Chen, M.** *et al.* (2023) Transcription factor CsMYB77 negatively regulates fruit ripening and fruit size in citrus. *Plant Physiology*, **194**, 867–883.

Zhang, X., **Ju, H.**, **Chung, M.**, **Huang, P.**, **Ahn, S.** & **Kim, C.** (2010) The R-R-type MYB-like transcription factor, AtMYBL, is involved in promoting leaf senescence and modulates an abiotic stress response in Arabidopsis. *Plant and Cell Physiology*, **52**, 138–148.

Zhao, M., **Lei, Y.**, **Wu, L.**, **Qi, H.**, **Song, Z.** & **Xu, M.** (2024) The miR159a-PeMYB33 module regulates poplar adventitious rooting through the abscisic acid signal pathway. *The Plant Journal*, **118**, 879–891.

Zhao, X., **Wang, Q.**, **Wang, D.**, **Guo, W.**, **Hu, M.X.**, **Liu, Y.** *et al.* (2023) PagERF81 regulates lignin biosynthesis and xylem cell differentiation in poplar. *Journal of Integrative Plant Biology*, **65**, 1134–1146.

Zhu, N., **Cheng, S.**, **Liu, X.**, **Du, H.**, **Dai, M.**, **Zhou, D.X.** *et al.* (2015) The R2R3-type MYB gene OsMYB91 has a function in coordinating plant growth and salt stress tolerance in rice. *Plant Science*, **236**, 146–156.